Supporting Information

The Exosome Total Isolation Chip (ExoTIC)

Fei Liu[1,2,3,4†], Ophir Vermesh[2,5†], Vigneshwaran Mani[1,2], Tianjia J. Ge[2,5], Steven J. Madsen[6], En-Chi Hsu[1,2], Gayatri Gowrishankar[2,5], Edwin Chang[1,2,5], Kaushik Sridhar[1,2], Abel Bermudez[1,2], Sharon J. Pitteri[1,2], Tanya Stoyanova[1,2], Robert Sinclair[6], Viswam S. Nair[1,2,7], Sanjiv S. Gambhir[1,2,5,6,8], and Utkan Demirci[1,2]**

AFFILIATIONS

[1]Canary Center at Stanford for Cancer Early Detection, Department of Radiology, School of Medicine, Stanford University, Stanford, CA 94304

[2]Department of Radiology, School of Medicine, Stanford University, Stanford, CA 94304

[3]School of Ophthalmology & Optometry, School of Biomedical Engineering, Wenzhou Medical University, Wenzhou, Zhejiang 325035, China

[4]Wenzhou Institute of Biomaterials and Engineering, Chinese Academy of Sciences, Wenzhou, Zhejiang 325001, China

[5]Molecular Imaging Program at Stanford, Radiology Department, School of Medicine, Stanford University, Stanford, CA 94304

[6]Department of Materials Science and Engineering, Stanford University, Stanford, CA 94304

[7]Department of Medicine, Stanford University, Stanford, CA 94304

[8]Department of Bioengineering, Stanford University, Stanford, CA 94304

[†] Fei Liu and Ophir Vermesh contributed equally to the work.

*Correspondence should be addressed to S. S. G. (sgambhir@stanford.edu) and U. D. (utkan@stanford.edu)

METHODS

Design, Materials, and Fabrication of the ExoTIC Device. The ExoTIC device has a pair of axial plates between which ring-like gaskets are captured that secure a membrane (as illustrated in Figure S1, a low protein binding filter membrane made from track-etched polycarbonate having a 30 nm or 50 nm pore size) and a polyethersulfone (PES) filter (as illustrated, 200 nm pore size) in place. The PES filter along with a supportive paper pad (positioned within the inner diameter of the gasket between the filter/membrane and back plate with the outlet) provide structural support for the membrane. A flow chamber is collectively defined between the walls of the plates and gaskets. One of the axial plates has an inlet opening, while the other has an outlet opening, with both the inlet opening connected to the flow chamber. The flow chamber is designed such that all fluid flowing from the inlet to the outlet must pass through the membrane, filter, and supportive paper pad. The central axes of the inlet and the outlet openings, as illustrated in Figure S2, are not coincident with one another; instead they are angularly offset from one another (as depicted, approximately 180 degrees from the central axis of the plates) creating some radial travel distance over which the flow of the sample will occur and eliminating a line of direct fluid pressure between the inlet and outlet openings. To create a strong, fluid-tight seal around the periphery, the plates are secured to one another by a ring of compressive fasteners (here, nine bolts and nuts) which encircle the circumference of flow chamber (Figure S1 and S2).

The various separate components of the ExoTIC device are illustrated at Figure S2c. As depicted in steps 1 and 2 of Figure S2d, one of the PMMA plates (the one with the outlet on) has fasteners inserted through it to form posts on which a plastic gasket was overlaid as shown in step 3. In step 4, the paper pad is inserted into the opening of the gasket to support the filter, such

that the back surface of the paper pad contacts the wall of the plate with the outlet opening. In step 5, the PES filter is laid down over the opening of the gasket, with the filter having a diameter slightly larger than the inner diameter of the gasket. The membrane is also laid down over the filter. In step 6, a second gasket is overlaid to capture the membrane and filter between the two gaskets. In steps 7 and 8, the opposing plate (with the inlet) is placed over the second gasket and nuts are threaded to the fasteners to compress the plates towards one another and form the assembled ExoTIC device.

Cell culture EV isolation and purification. The U87 GBM (glioblastoma) cell line was cultured in DMEM (Life Technologies), supplemented with 10% fetal bovine serum (HyClone; Perbio Sciences) and penicillin-streptomycin antibiotic (Life Technologies). Three cell lines, HCC827 (human lung adenocarcinoma), H1650 (non-small cell lung cancer), and 22Rv1 (prostate cancer) were cultured in RPMI-1640 media (Gibco), supplemented identically to DMEM with the addition of sodium pyruvate (100 mM, Life Technologies). Each cell line was routinely tested for mycoplasma and treated prophylactically with Plasmocin^{TM} (InvivoGen) to prevent contamination with mycoplasma EVs and RNA. Cell lines were monitored closely for confluence and cell death, and were replaced by thawing a new frozen vial every 1-2 months. For maintenance, cells were passaged weekly by seeding 400,000 cells in a 75 cm^2 cell culture flask (Corning) until confluent. For EV isolation, each cell type was seeded at 300,000 cells in separate wells of a 6-well cell culture plate (Corning Costar). Once the well reached ~80% confluence, ~2 days after seeding (depending on cell type), culture media was aspirated from each well and replaced with media supplemented with serum-free media. After 48 hours, media from each cell type was collected and centrifuged at 1,500 g for 10 minutes to pellet large debris or cells. Supernatants were passed through a 0.22 μm PES filter (Millipore). The resulting

solution then underwent one of four different isolation protocols for EV isolation. In certain instances (*e.g.* for miRNA comparison analysis), trypsin was added to the wells to detach and pellet cells for subsequent analysis.

Profiling the EV size and quantity of EVs isolated by ExoTIC device. EV samples isolated by one of the four methods previously indicated were analyzed by nanoparticle tracking analysis (NTA) (Nanosight NS300, Malvern Instruments Limited) to determine size distribution and concentration. To disaggregate any EV aggregates, samples were warmed to room temperature and vortexed before being serially diluted to achieve the recommended ~ 30−100 particles/frame in the on-screen video display. For EV samples prepared from cell culture media, a 10-μL volume of EV solution was diluted 100−fold for NTA analysis. For the EV samples prepared from plasma, a 10 μL volume of plasma EV solution was diluted 500−fold for NTA analysis. Software parameters were adjusted to give a bin size of 1 nm, a line jump distance of 16, and a target temperature of 25°C. A series of washes with ethanol and PBS were performed between each sample run. Data analysis was performed in triplicate and exported as an Excel file containing the data points, a PDF file of the size distribution and concentration graphs, and video recordings for each sample. Total number of exosomes was calculated by multiplying the volume of enriched sample and the concentration (EVs/mL) from Nanosight. The total sample volume of media/plasma/lavage that was used for exosome processing was accounted, and data is presented as EVs per mL of raw media, plasma or lavage.

EV scanning electron microscopy. Preparation of PLLA-coated silicon substrate: A 100 μL polyL-lysine (PLLA) solution (0.1 mg/ mL in 1X PBS) was pipetted into a well of a 48−well plate containing a silicon substrate (5 × 7 mm, TED PELLA, INC.) and incubated overnight at 4^{o}C. The silicon substrate was then washed three times with 500 μL of 1X PBS. Sample Fixation:

100 μL of EVs (in PBS) was pipetted onto the surface of PLLA-coated silicon substrates and incubated at 4 ^{o}C overnight to allow the EVs time to settle onto the surface of the silicon substrate. Then the EV solution was removed (while avoiding drying). 2% glutaraldehyde with 4 % PFA in 0.1 M sodium cacodylate buffer (pH 7.3) was added and incubation proceeded at 4 ^{o}C for 30 min to allow the EVs time to settle onto the surface of the silicon substrate. Post−Fixation: Two substitutions of 0.1M sodium cacodylate containing 1% aq. OsO_4 was used to stain and further fix the EVs, followed by three washes with mQ−H_2O. Dehydration: Substrates were incubated in successively higher ethanol concentrations (50%, 70%, and 90% EtOH, 5min each) followed by steps washes with 100% EtOH, 5min each at room temperature. Drying: A critical point dryer (CPD) chamber was filled with 100% EtOH, the sample was placed in the chamber, and the machine was operated as per the instrument manual. SEM images of EVs were acquired using the Zeiss Sigma FESEM instrument at the Beckman Center at Stanford.

EV transmission electron microscopy. Preparation for TEM analysis was based on a modified version of previously published protocols.[1] Carbon coated copper grids (Ted Pella Inc.) were glow discharged. All solutions were applied to the membrane-coated side of the grids. This side was kept wet for sample preparation steps, while the reverse side was kept dry. Isolated exosomes were mixed with an equal volume of 4% paraformaldehyde. Then, a 5 μL drop of the fixed EV solution was placed on the TEM grid and allowed to incubate for 20 minutes while covered. Next, samples were washed and blocked by placing each one face down on top of 100 μL drops of the following solutions: PBS (2X, 3 minutes each), PBS / 50 mM glycine (4X, 3 min.), PBS / 5% BSA (1X, 10 min.). A 20 μg/ml solution of mouse anti-human CD63 antibody Clone TS63 (Abcam) was used for labeling (1 hour), followed by six washes in PBS / 0.5% BSA. Samples were incubated in a 1:50 dilution of rabbit anti-mouse immunogold conjugate (Sigma)

in 5% BSA / PBS (20 min.) and washed in PBS (6X) followed by water (6X). Finally, negative staining of the samples was achieved using a 1:9 ratio mixture of 2% methylcellulose and 4% uranyl acetate (10 min.). Excess liquid was wicked away using Whatman No. 1 filter paper, leaving a thin film behind to dry. Imaging was performed in an FEI Tecnai TEM operated at 200 kV.

Flow model through pores in Whatmann filter membrane

The pressure drop through porous membrane was analyzed based on the Weissberg-Sampson-Poiseuille approximation.[2] Essentially, all the inertial effects in the system are neglected and the fluid is assumed to undergo an incompressible Stokes flow.

Initially, the flow through an infinitely thin circular pore is estimated under the conditions pertaining to a Sampson flow:

$$\Delta P = \frac{3\mu q}{a^3}$$

where ΔP is the pressure drop across the pore and μ is the shear viscosity of the sample which is used to isolate the exosomes. Plasma samples were used to approximate the shear viscosity in this case. Assuming a parallel coupling of the pores the individual flow rates can be expressed as a combination of the macroscopic volumetric flow rate and the number of pores.

$$\Delta P = \frac{3\mu Q}{Na^3}$$

$$a = 0.025\ um, Q = \frac{5mL}{hr}, \mu = 1.2\ mPa.sec, N = 6\ x\ 10^8$$

Substituting these values, the pressure drop is estimated to be 0.530 kPa. In the parallel coupling configuration, the pressure drop across each pore is identical.

Since the thickness of the membrane used is much greater than the radius of the pore, we include the Hagen-Poiseuille equation[3] to estimate the pressure drop across the thickness of the membrane. In this case the pressure drop is estimated by:

$$\Delta P = \frac{8\mu t Q}{N\pi a^4}$$

where the thickness of the membrane is $8\,\mu m$. Thus the pressure drop is calculated to be 144 kPa.

Thus the total pressure drop across the pore of the membrane can be assumed to be a linear combination of the Sampson and Poiseuille flow though the error accrued by the linear summation of these flows are greatest when the thickness is twice the pore radius but is less than 1% for all other cases.[4]

Pressure exerted due to ultracentrifugation:

The pressure exerted on the cell bodies due to the ultracentrifugation process can be divided into various components, namely – centrifugal g−force, viscous drag force, increased cell 'weight', hydrostatic pressure due to liquid head & the cell pellet pressure. Of these, the maximum pressure on cell bodies was derived from the hydrostatic pressure exerted by the liquid on the cells when deposited at the bottom of the centrifuge.[5]

Hence, neglecting all other factors such as the variable density of the liquid head in different regions of the column & varying drag force, the hydrostatic pressure is related to the cell radius as given by:[6]

$$P = \omega^2 \rho (r_0 h + \frac{h^2}{2})$$

where P is hydrostatic pressure,

ω *is the angular velocity,* ρ *is density of liquid,* r_0 *is the radial distance fro m the axis of rotation*

& h is the height of the liquid column above the cell pellet.

In our experiments, a fixed angle rotor (TX865) was used to run the WX Sorvall ultracentrifuge. The numerical values used here are:

$$\omega = 60{,}000\ rpm$$

$$\rho = 1\ g/mL$$

$$r_0 = 9.10\ cm$$

$$h = 14\ mm$$

Substituting these values, the pressure obtained at the bottom of the column is found to be ~542 atm or 54918 kPa.

Thus, the pressures experienced by the cell bodies in an ultracentrifuge is approximately 380 times greater than that in a porous membrane.

ExoTIC for processing larger volumes of samples

At flow rates >5mL/hr, the back pressure becomes too high for ExoTIC devices with 30 nm and 50 nm pore sizes, causing our pump to stall. Smaller pores and higher flow rates increase the pressure drop across the membrane, as given by the equation $\Delta P = 3\mu Q/Nr^3$, where ΔP is pressure drop, μ= shear viscosity, r = pore radius, and N= number of pores. Increasing the flow rate from 5mL/hr to 10mL/hr doubles the pressure drop from 0.5 kPa to 1kPa, exceeding the power of our pump motor. While 5mL/hr may be the upper limit of flow rate for our pump, we have not yet tried other syringe pump brands, which may have stronger motors and be capable of higher flow rates. However, multiple ExoTIC devices can be run in parallel on the same syringe pump, as each pump can hold up to 6 syringes (Figure S3) and multiple syringe pumps can be run simultaneously. In principle, a 100 mL sample could be run with several devices in parallel, each containing 10−15 mL of sample, permitting processing within 2−3 hours. In addition, due to the higher yields achievable with ExoTIC, a fraction of the volume used in UC can be processed to obtain the same total exosome count, relaxing the requirement for large sample volumes.

Therefore, taking into all these issues, we optimized all our ExoTIC devices experiments with 5mL/hr.

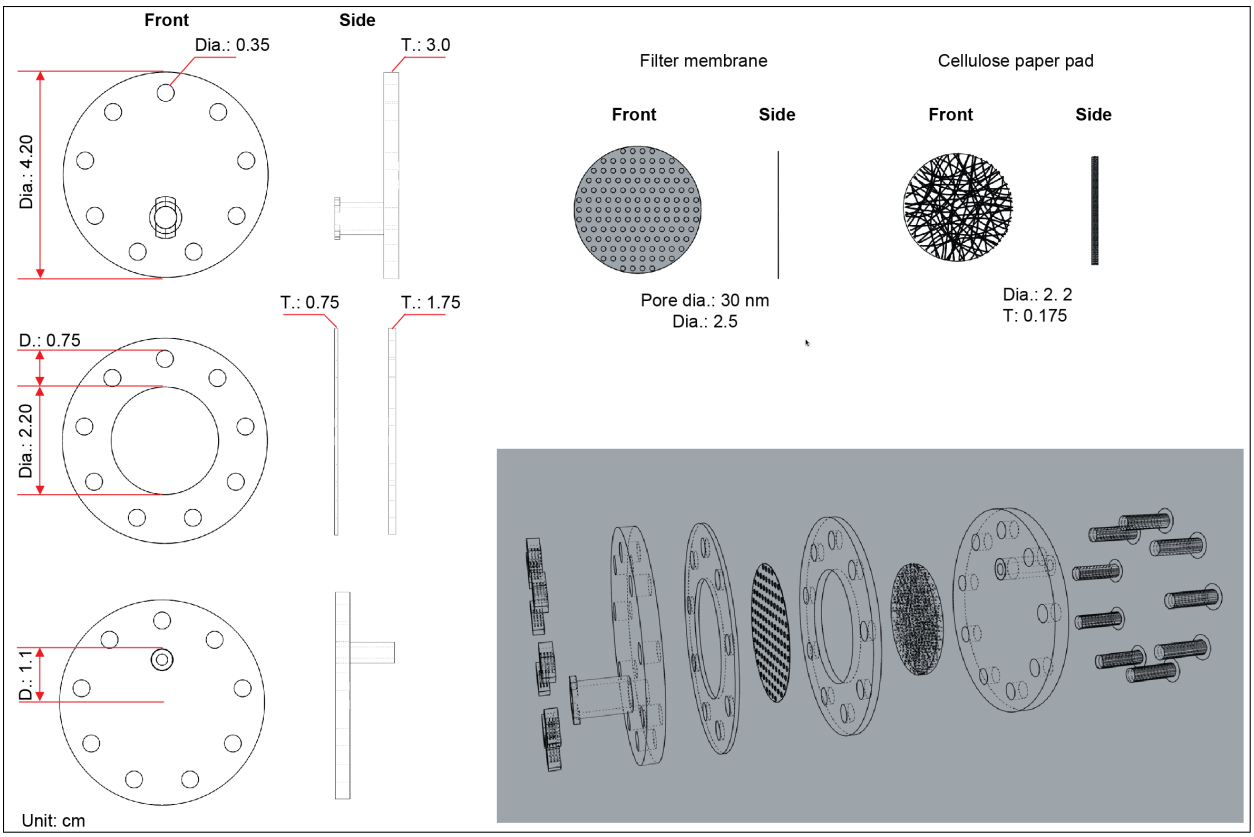

Figure S1. Design and features of ExoTIC device.

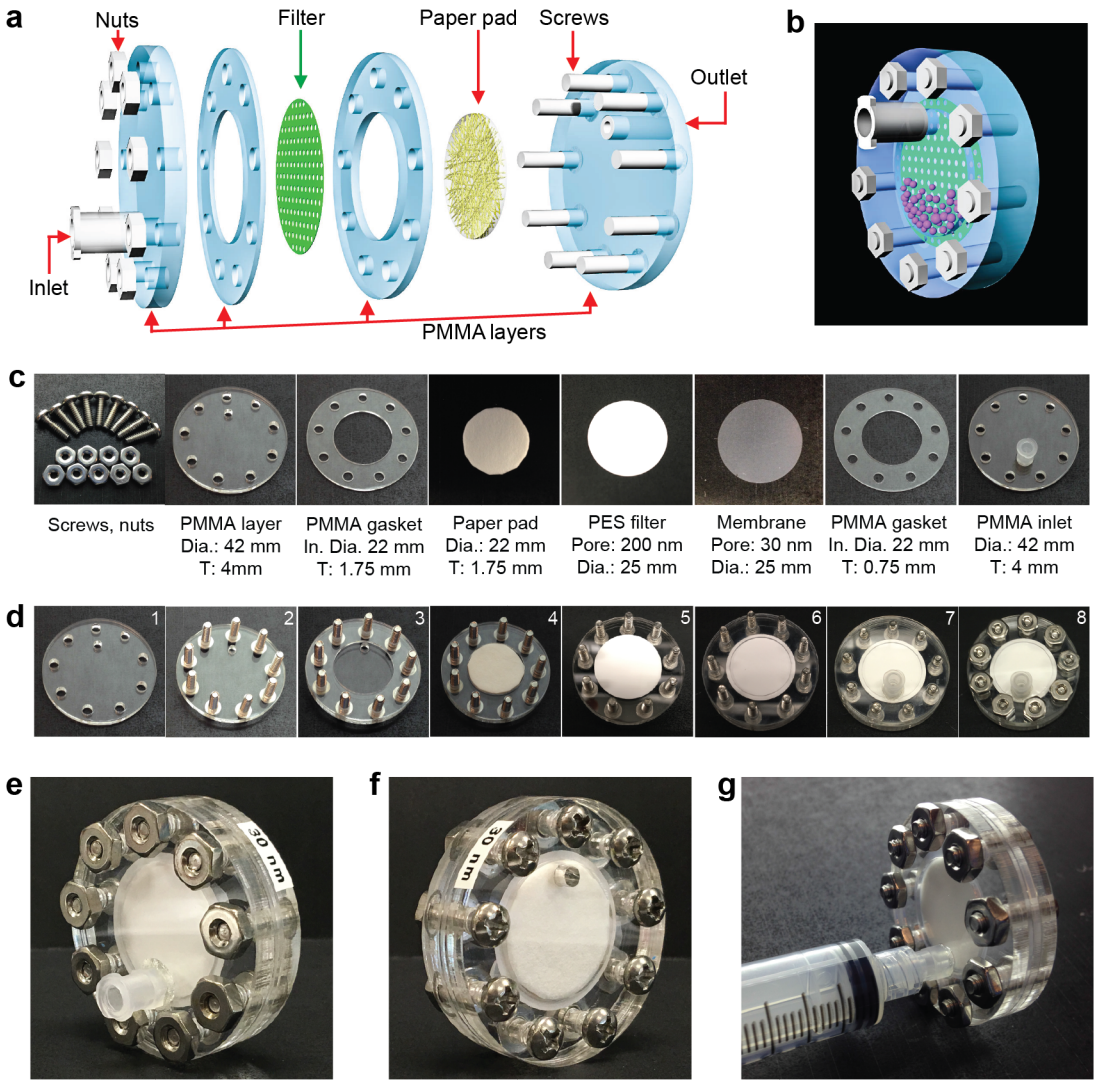

Figure S2. Materials and fabrication process of ExoTIC device. (a) Schematic illustration of the different layers of ExoTIC device. (b) Schematic of assembled ExoTIC device. (c) The picture of materials used for fabrication of ExoTIC device. (d) The fabrication procedure of ExoTIC device. (e), (f) and (g) pictorial representation of the front, back and syringe collected ExoTIC device.

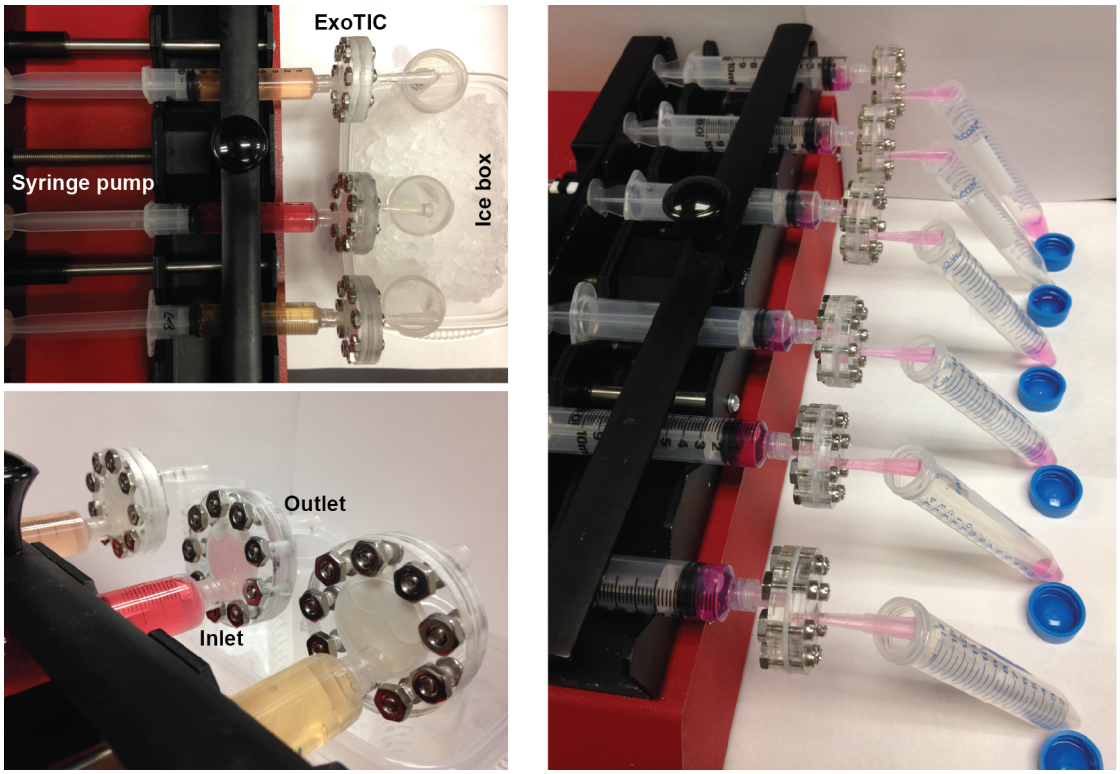

Figure S3. ExoTIC devices for parallel isolation of EVs from multiple samples.

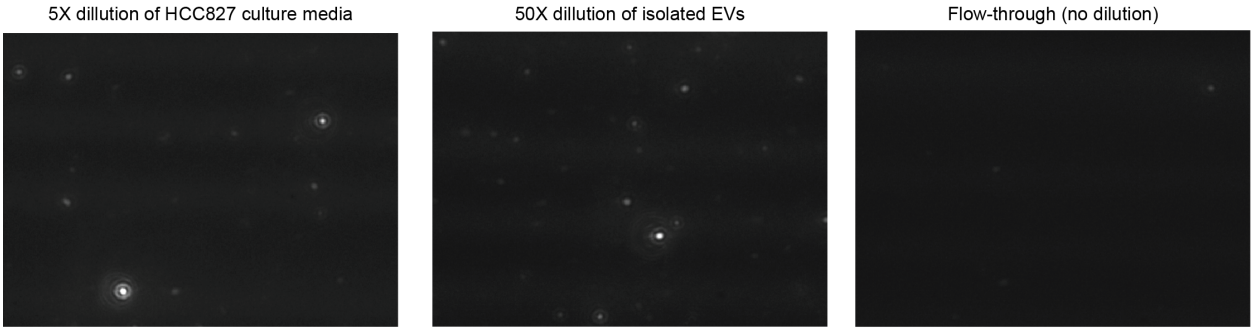

$$\text{Recovery Efficiency} = \frac{\text{Total amount of isolated EVs}}{\text{Total amount of EVs in culture media before isolation}} \times 100\%$$

$$= \sim 92\ \%$$

Figure S4. Estimation the EV isolation efficiency of ExoTIC device. The culture media of cancer cells was filtered with a 200nm PES syringe filter to remove everything larger than 200 nm. Then the filtered culture media (3 mL) was 5X diluted in 1XPBS for analysis with Nanosight. Then same volume of culture media was applied with ExoTIC to isolate EVs. The total amount of EVs isolated by ExoTIC was also characterized with Nanosight. Therefore, estimation on the EV isolation efficiency was calculated as the percentage of (total amount of EVs isolated using ExOTIC)/ (Total amount of EVs in culture media before isolation).

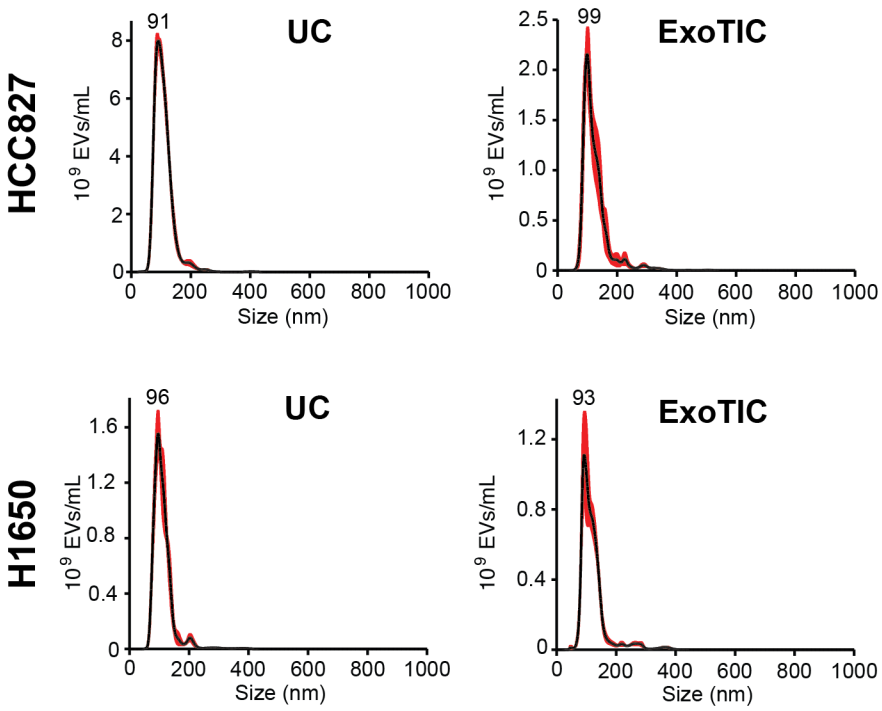

Figure S5. UC *vs*. ExoTIC for EV isolation. Isolated EVs using UC compared to ExoTIC device are shown in two cancer cell lines HCC 827 (Lung) and H1850 (Lung).

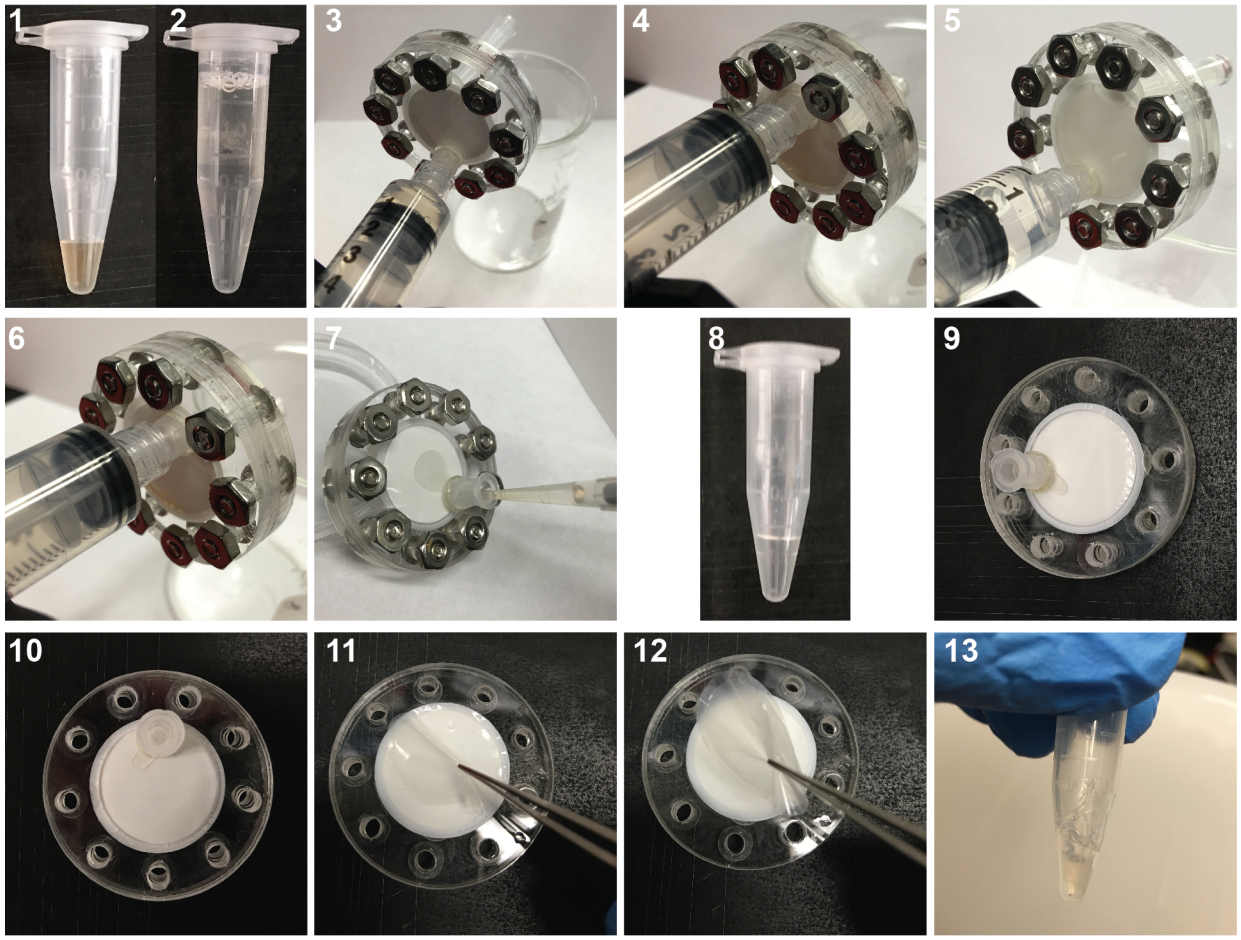

Figure S6. Process of EV isolation from plasma. 1) 100 µL plasma in a 1.5 mL microtube. 2) 10X diluted plasma in PBS. 3) and 4) EV isolation. 5) and 6) 1X PBS washing. 7) Pipetting the enriched EVs from the inlet. 9) to 11) Disassembled ExoTIC device. 12 and 13) Collection of the filter membrane and insertion into the enriched EV media.

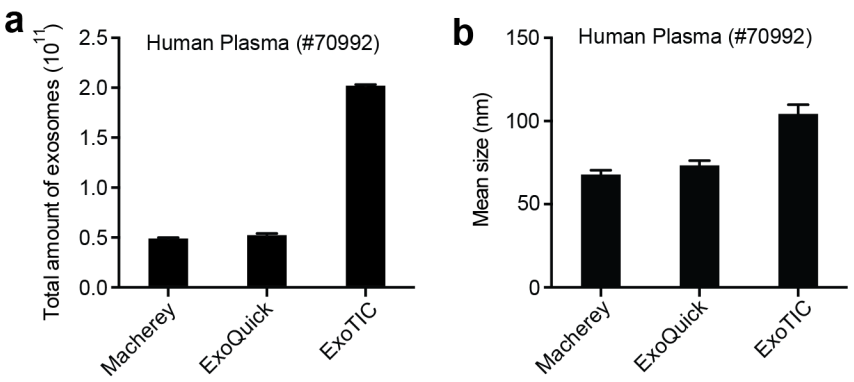

Figure S7. ExoTIC device for isolation of EVs from healthy human plasma samples. (a) Yield comparison of EV yield isolated from two different 100 μL healthy human plasma samples. (b) Mean sizes of human plasma EVs isolated using various isolation methods.

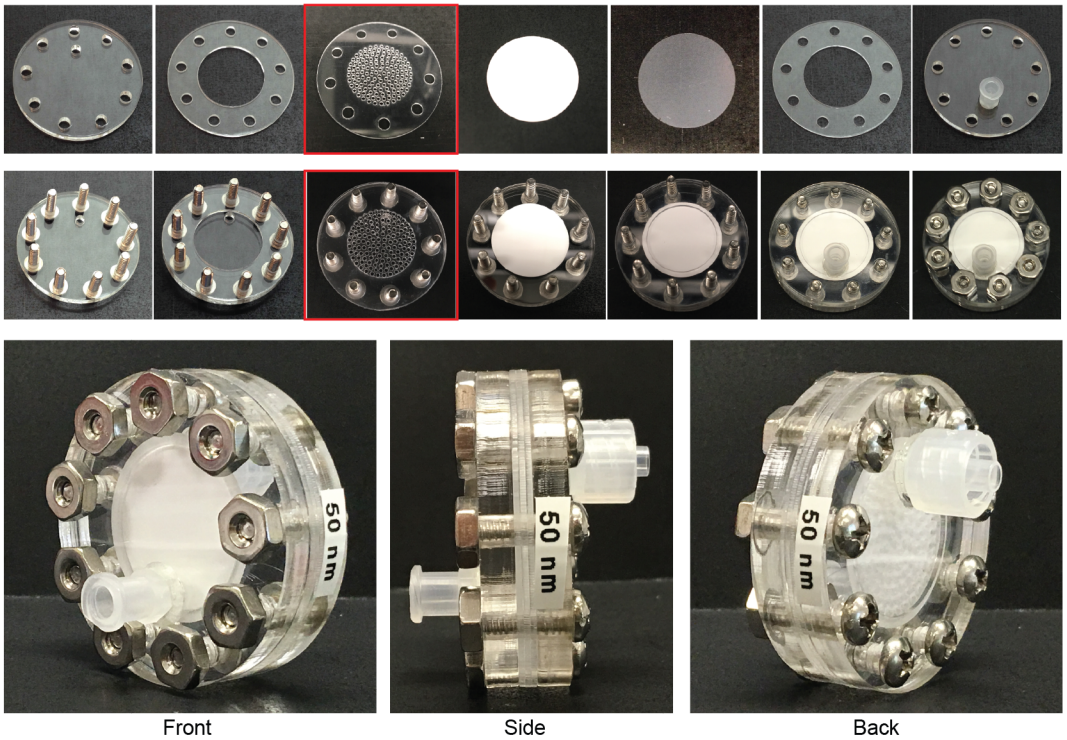

Figure S8. Design and fabrication of a building block of the ExoTIC device for modular function.

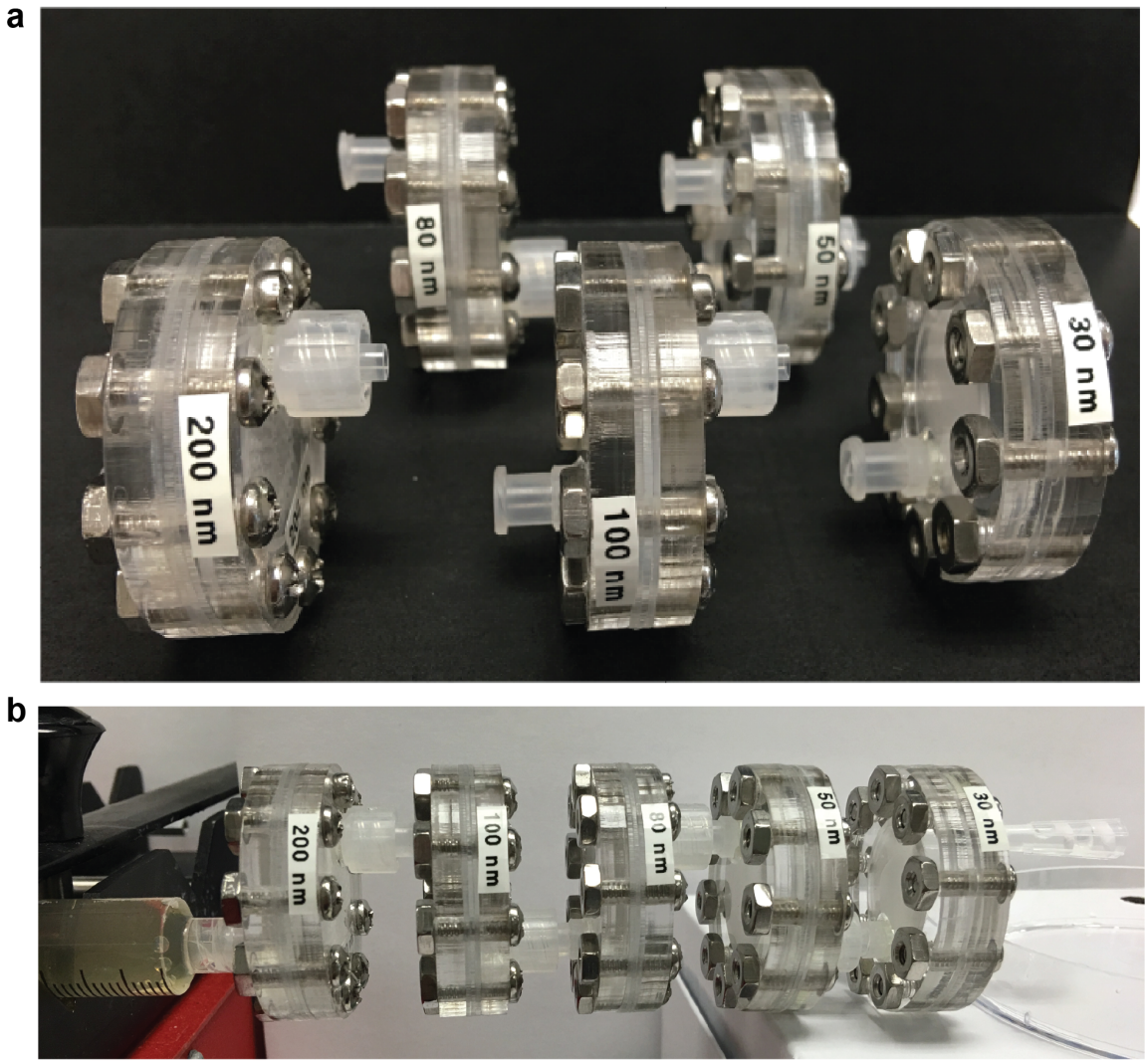

Figure S9. Serial connection of ExoTIC device for size-based EV separation from heterogeneous sized EV populations.

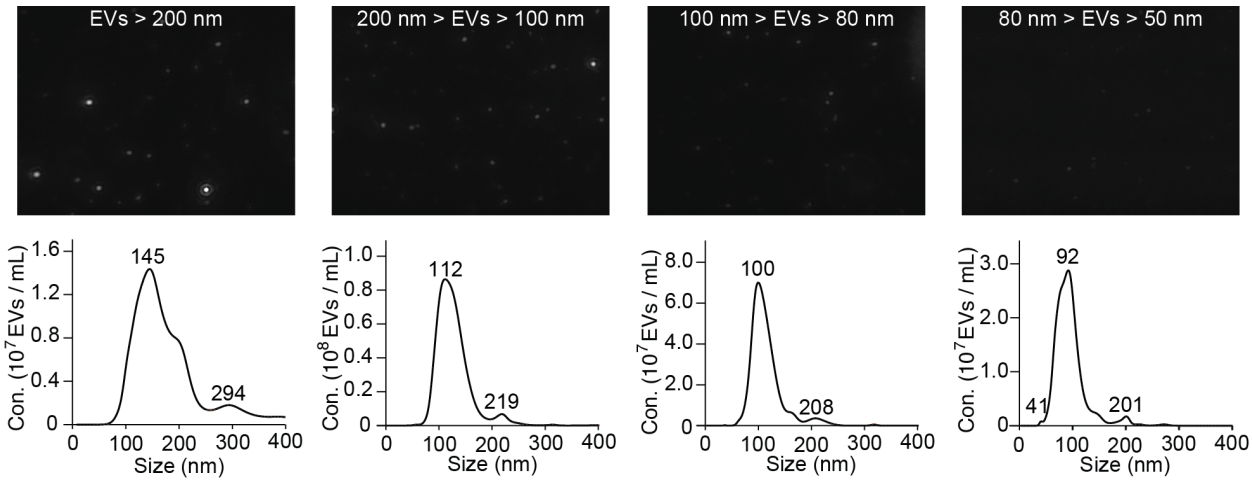

Figure S10. Size distribution (by nanoparticle tracking analysis) of HCC827 EVs isolated from each of the specific pore sized ExoTIC device connected in series.

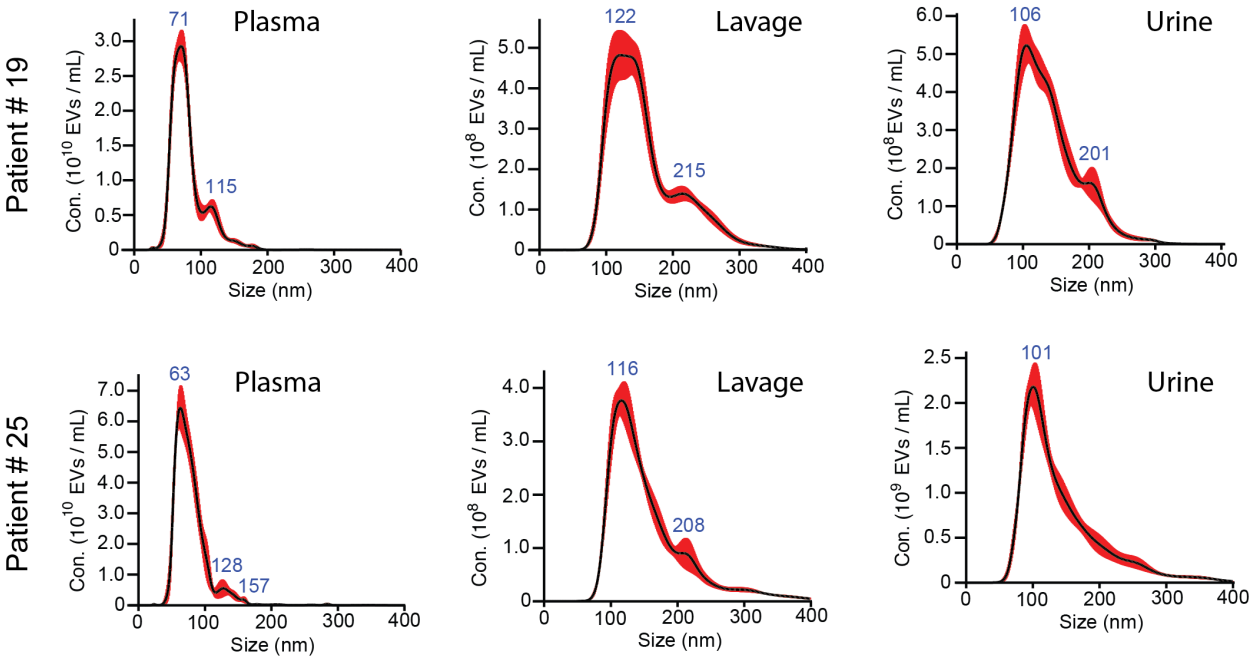

Figure S11. Analysis of EVs isolated from different types of clinical samples. Lavage = Bronchoalveolar Lavage.

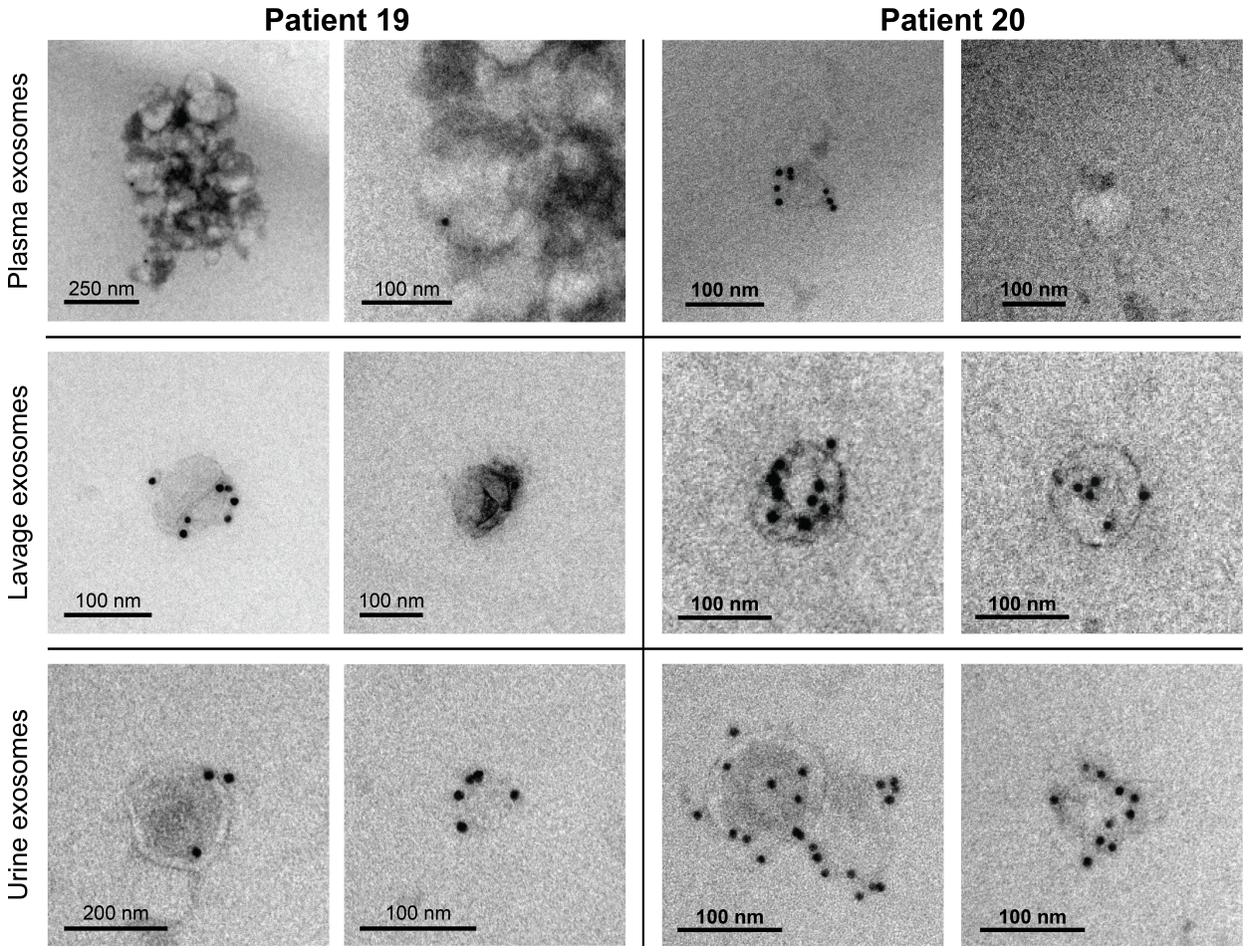

Figure S12. TEM characteristics of EVs using immuno-GNP-CD63 (GNP dia. 10 nm) antibody. EVs isolated from plasma, bronchoalveolar lavage and urine samples of patients 19 and 20.

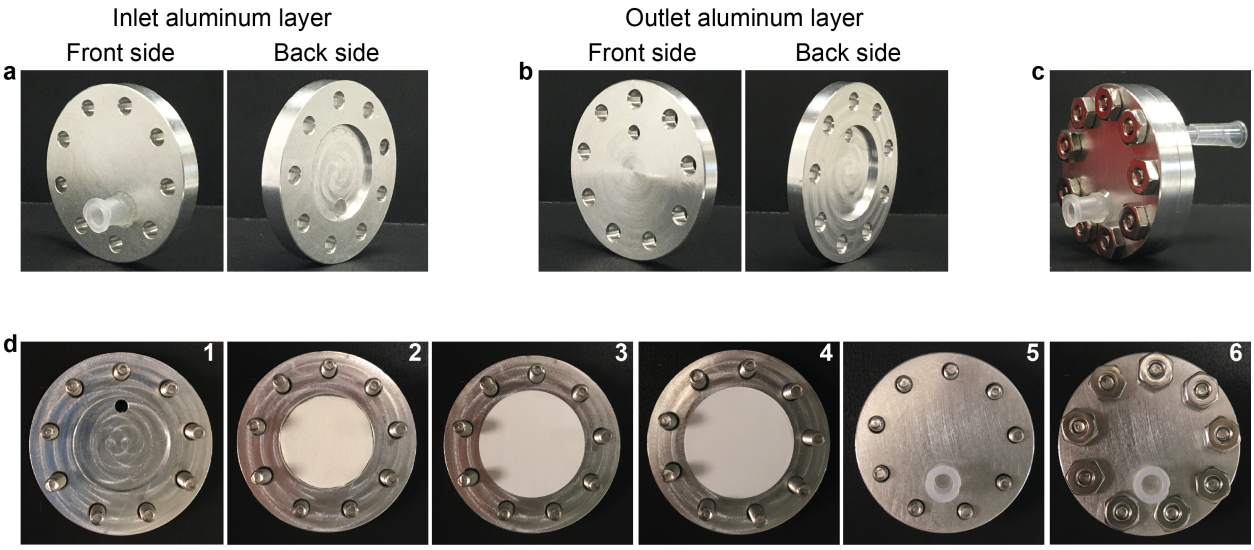

Figure S13. Fabrication of metal ExoTIC device using aluminum.

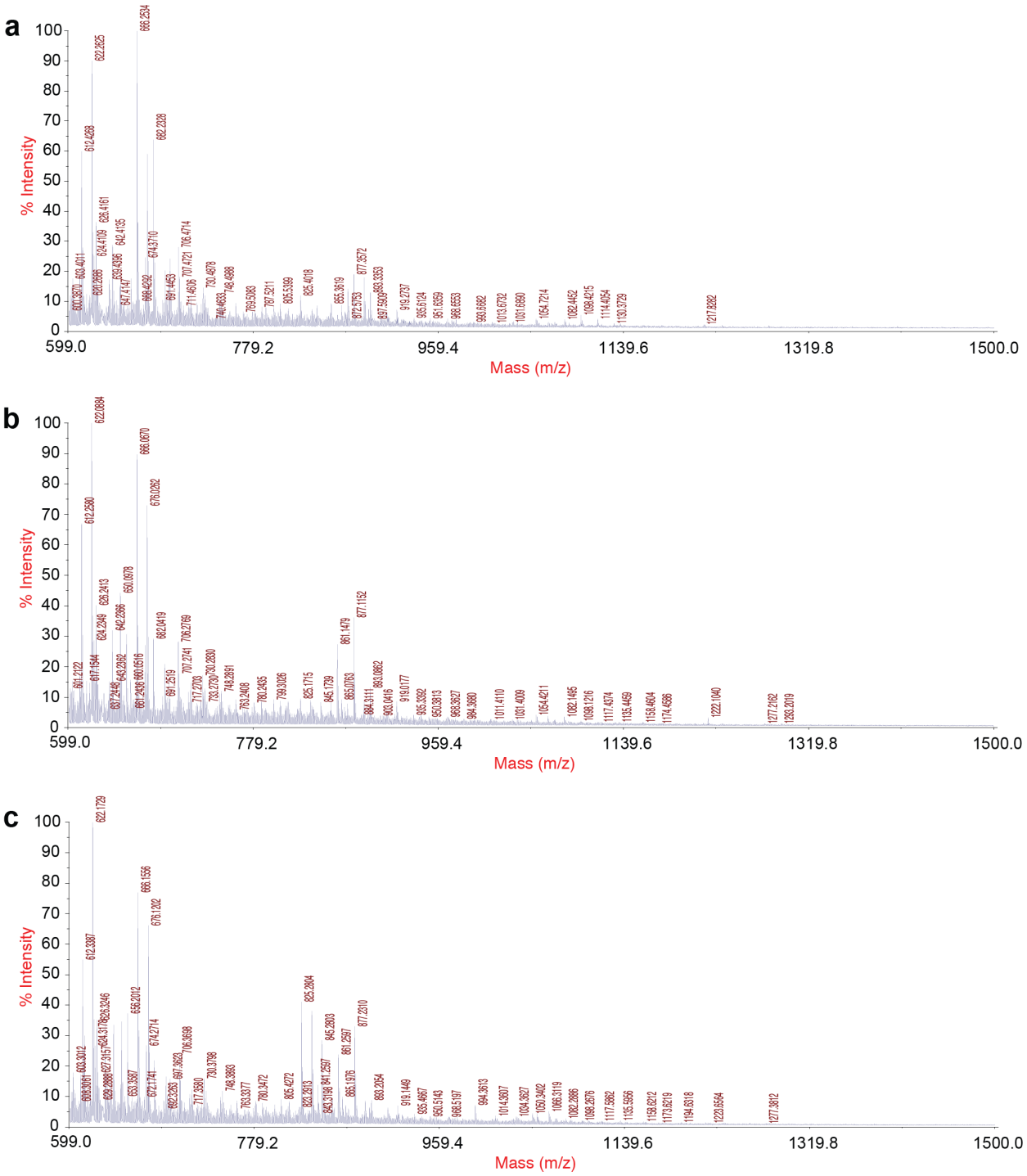

Figure S14. Mass spectrum of polymer contaminant testing of plastic ExoTIC (P-ExoTIC) and aluminum ExoTIC (Al-ExoTIC) by flowing 10 mL of 10% acrylonitrile DI water solution with a flow rate of 5 mL/h. Compared with standard solution (a), both the PMMA made ExoTIC (b)

and aluminum made ExoTIC (c) do not show any contaminants from the materials we used for device fabrication.

Table S1. Quantification of microRNA between ExoTIC and UC using bioanalyzer.

Method	Cell line	EV amount	Concentration (ng/μL)
ExoTIC device (10 mL)	HCC827	3.75×10^{10}	100
	H1650	1.78×10^{10}	90
Ultracentrifugation (60 mL)	HCC827	5.85×10^{10}	100
	H1650	1.00×10^{10}	100

Table S2. Top 40 high expressed microRNAs list from Nanostring. (http://mircancer.ecu.edu/ http://www.mirbase.org/).

Official symbol	Target sequence	Family/cluster cancer
HCC827 (UC and ExoTIC) and H1650 (UC and ExoTIC)		
hsa-mir-1246	AAUGGAUUUUUGGAGCAGG	non-small cell lung cancer; cervical cancer; colorectal cancer; lung cancer
hsa-mir-134	UGUGACUGGUUGACCAGAGGGG	non-small cell lung cancer; colorectal cancer; endometrial cancer; gastric cancer; glioma; bead and neck squamous cell carcinoma; hepatocellular carcinoma; osteosarcoma; renal cell carcinoma
hsa-mir-145-5p	GUCCAGUUUUCCCAGGAAUCCCU	colorectal cancer; gastric cancer; hepatocellular carcinoma
hsa-mir-192-5p	CUGACCUAUGAAUUGACAGCC	
hsa-mir-22-3p	AAGCUGCCAGUUGAAGAACUGU	hepatocellular carcinoma
hsa-mir-25-3p	CAUUGCACUUGUCUCGGUCUGA	
hsa-mir-302d-3p	UAAGUGCUUCCAUGUUUGAGUGU	
hsa-mir-4531	AUGGAGAAGGCUUCUGA	
hsa-mir-579	UUCAUUUGGUAUAAACCGCGAUU	
HCC827 (ExoTIC)		
hsa-mir-2116-5p	GGUUCUUAGCAUAGGAGGUCU	
hsa-mir-378e	ACUGGACUUGGAGUCAGGA	
hsa-mir-520d-5p hsa-mir-518a-5p hsa-mir-527	CUACAAAGGGAAGCCCUUUC CUGCAAAGGGAAGCCCUUUC CUGCAAAGGGAAGCCCUUUC	
HCC827 (UC)		
hsa-mir-451a	AAACCGUUACCAUUACUGAGUU	breast cancer; hypopharyngeal squamous cell carcinoma; papillary thyroid cancer
hsa-mir-	CGAAAACAGCAAUUACCUUUGC	

570-3p		
HCC827 (UC and ExoTIC)		
hsa-mir-100-5p	AACCCGUAGAUCCGAACUUGUG	esophageal adenocarcinoma; gastric cancer
hsa-mir-574-5p	UGAGUGUGUGUGUGUGAGUGUGU	colorectal cancer
hsa-mir-720	UCUCGCUGGGGCCUCCA	acute myeloid leukemia; breast cancer; cervical cancer; colorectal cancer
HCC827 (UC and ExoTIC) and H1650 (UC)		
hsa-mir-188-3p	CUCCCACAUGCAGGGUUUGCA	
HCC827 (UC) and H1650 (UC and ExoTIC)		
hsa-mir-144-3p	UACAGUAUAGAUGAUGUACU	glioma; renal cell carcinoma
hsa-mir-15a-5p	UAGCAGCACAUAAUGGUUUGUG	hepatocellular carcinoma
HCC827 (ExoTIC) and H1650 (UC)		
hsa-mir-338-3p	UCCAGCAUCAGUGAUUUUGUUG	non-small cell lung cancer; colorectal cancer; gastric cancer; glioma; hepatocellular carcinoma; liver cancer; neuroblastoma;
H1650 (UC and ExoTIC)		
hsa-mir-489	GUGACAUCACAUAUACGGCAGC	breast cancer
H1650 (ExoTIC)		
hsa-mir-130a-3p	CAGUGCAAUGUUAAAAGGGCAU	
hsa-mir-191-5p	CAACGGAAUCCCAAAAGCAGCUG	
hsa-mir-23a-3p	AUCACAUUGCCAGGGAUUUCC	

Official symbol	**Target sequence**	**Family/cluster cancer**
hsa-mir-10a-5p	UACCCUGUAGAUCCGAAUUUGUG	
hsa-mir-149-5p	UCUGGCUCCGUGUCUUCACUCCC	Renal cell carcinoma
hsa-mir-155-5p	UUAAUGCUAAUCGUGAUAGGGGU	Colorectal carcinoma; gastric cancer
hsa-mir-16-5p	UAGCAGCACGUAAAUAUUGGCG	Non-small cell lung cancer
hsa-mir-1972	UCAGGCCAGGCACAGUGGCUCA	
hsa-mir-	CAGGCAGUGACUGUUCAGACGUC	

2682-5p		
hsa-mir-302e	UAAGUGCUUCCAUGCUU	
hsa-mir-320e	AAAGCUGGGUUGAGAAGG	
hsa-mir-367-3p	AAUUGCACUUUAGCAAUGGUGA	
hsa-mir-4454	GGAUCCGAGUCACGGCACCA	
hsa-mir-4455	AGGGUGUGUGUGUUUUU	
hsa-mir-514b-5p	UUCUCAAGAGGGAGGCAAUCAU	
hsa-mir-548aa	AAAAACCACAAUUACUUUUGCACCA	
hsa-mir-548ai	AAAGGUAAUUGCAGUUUUUCCC	
hsa-mir-549	UGACAACUAUGGAUGAGCUCU	
hsa-mir-612	GCUGGGCAGGGCUUCUGAGCUCCUU	Hepatocellular carcinoma

Table S3. The list of peptides identified by LC-MS/MS of EVs from 22RV1 cells.

(www.oncomine.org; www.microvesicles.org; www.evpedia.info; www.exocarta.org)

Gene Name	**Protein Name**	
ATP1A1*	Sodium/potassium-transporting ATPase subunit alpha-1 (Na(+)/K(+) ATPase alpha-1 subunit) (EC 3.6.3.9) (Sodium pump subunit alpha-1)	
CCDC50*	Coiled-coil domain-containing protein 50 (Protein Ymer)	
CCT3*	T-complex protein 1 subunit gamma (TCP-1-gamma) (CCT-gamma) (hTRiC5)	
CCT4*	T-complex protein 1 subunit delta (TCP-1-delta) (CCT-delta) (Stimulator of TAR RNA-binding)	
CCT5*	T-complex protein 1 subunit epsilon (TCP-1-epsilon) (CCT-epsilon)	
CCT8*	T-complex protein 1 subunit theta (TCP-1-theta) (CCT-theta) (Renal carcinoma antigen NY-REN-15)	
CD63*	CD63 antigen (Granulophysin) (Lysosomal-associated membrane protein 3) (LAMP-3) (Melanoma-associated antigen ME491) (OMA81H) (Ocular melanoma-associated antigen) (Tetraspanin-30) (Tspan-30) (CD antigen CD63)	
CD9*	CD9 antigen (5H9 antigen) (Cell growth-inhibiting gene 2 protein)	

	(Leukocyte antigen MIC3) (Motility-related protein) (MRP-1) (Tetraspanin-29) (Tspan-29) (p24) (CD antigen CD9)	
CD99*	CD99 antigen (12E7) (E2 antigen) (Protein MIC2) (T-cell surface glycoprotein E2) (CD antigen CD99)	
CLTC*	Clathrin heavy chain 1 (Clathrin heavy chain on chromosome 17) (CLH-17)	
CLU*	Clustered mitochondria protein homolog	
EIF5A*	Eukaryotic translation initiation factor 5A-1 (eIF-5A-1) (eIF-5A1) (Eukaryotic initiation factor 5A isoform 1) (eIF-5A) (Rev-binding factor) (eIF-4D)	
EPCAM*	Epithelial cell adhesion molecule (Ep-CAM) (Adenocarcinoma-associated antigen) (Cell surface glycoprotein Trop-1) (Epithelial cell surface antigen) (Epithelial glycoprotein) (EGP) (Epithelial glycoprotein 314) (EGP314) (hEGP314) (KS 1/4 antigen) (KSA) (Major gastrointestinal tumor-associated protein GA733-2) (Tumor-associated calcium signal transducer 1) (CD antigen CD326)	
FASN*	Fatty acid synthase (EC 2.3.1.85) [Includes: [Acyl-carrier-protein] S-acetyltransferase (EC 2.3.1.38); [Acyl-carrier-protein] S-malonyltransferase (EC 2.3.1.39); 3-oxoacyl-[acyl-carrier-protein] synthase (EC 2.3.1.41); 3-oxoacyl-[acyl-carrier-protein] reductase (EC 1.1.1.100); 3-hydroxyacyl-[acyl-carrier-protein] dehydratase (EC 4.2.1.59); Enoyl-[acyl-carrier-protein] reductase (EC 1.3.1.39); Oleoyl-[acyl-carrier-protein] hydrolase (EC 3.1.2.14)]	
H2AFV*	Histone H2A.V (H2A.F/Z)	
H2AFX*	Histone H2AX (H2a/x) (Histone H2A.X)	
HIST1H1B*	Histone H1.5 (Histone H1a) (Histone H1b) (Histone H1s-3)	
HIST1H1E*	Histone H1.4 (Histone H1b) (Histone H1s-4)	
HIST1H2BB*	Histone H2B type 1-B (Histone H2B.1) (Histone H2B.f) (H2B/f)	
HIST1H2BC*	Histone H2B type 1-C/E/F/G/I (Histone H2B.1 A) (Histone H2B.a) (H2B/a) (Histone H2B.g) (H2B/g) (Histone H2B.h) (H2B/h) (Histone H2B.k) (H2B/k) (Histone H2B.l) (H2B/l)	
HIST3H3*	Histone H3.1t (H3/t) (H3t) (H3/g)	
IGSF8*	Immunoglobulin superfamily member 8 (IgSF8) (CD81 partner 3) (Glu-Trp-Ile EWI motif-containing protein 2) (EWI-2) (Keratinocytes-associated transmembrane protein 4) (KCT-4) (LIR-D1) (Prostaglandin regulatory-like protein) (PGRL) (CD antigen CD316)	
KHSRP	Far upstream element-binding protein 2 (FUSE-binding protein 2) (KH type-splicing regulatory protein) (KSRP) (p75)	
LAMA5*	Laminin subunit alpha-5 (Laminin-10 subunit alpha) (Laminin-11 subunit alpha) (Laminin-15 subunit alpha)	
LGALS3BP*	Galectin-3-binding protein (Basement membrane autoantigen p105) (Lectin galactoside-binding soluble 3-binding protein) (Mac-2-binding protein) (MAC2BP) (Mac-2 BP) (Tumor-associated antigen 90K)	

MMP14*	Matrix metalloproteinase-14 (MMP-14) (EC 3.4.24.80) (MMP-X1) (Membrane-type matrix metalloproteinase 1) (MT-MMP 1) (MTMMP1) (Membrane-type-1 matrix metalloproteinase) (MT1-MMP) (MT1MMP)	
MVB12A*	Multivesicular body subunit 12A (CIN85/CD2AP family-binding protein) (ESCRT-I complex subunit MVB12A) (Protein FAM125A)	
PABPC1*	Polyadenylate-binding protein 1 (PABP-1) (Poly(A)-binding protein 1)	
PACSIN3*	Protein kinase C and casein kinase substrate in neurons protein 3 (SH3 domain-containing protein 6511)	
PCBP2*	Poly(rC)-binding protein 2 (Alpha-CP2) (Heterogeneous nuclear ribonucleoprotein E2) (hnRNP E2)	
PDCD6IP*	Programmed cell death 6-interacting protein (PDCD6-interacting protein) (ALG-2-interacting protein 1) (ALG-2-interacting protein X) (Hp95)	
PSMA7*	Proteasome subunit alpha type-7 (EC 3.4.25.1) (Proteasome subunit RC6-1) (Proteasome subunit XAPC7)	
RAB5C*	Ras-related protein Rab-5C (L1880) (RAB5L)	
RPL29*	60S ribosomal protein L29 (Cell surface heparin-binding protein HIP)	
TSG101*	Tumor susceptibility gene 101 protein (ESCRT-I complex subunit TSG101)	
VPS37B*	Vacuolar protein sorting-associated protein 37B (hVps37B) (ESCRT-I complex subunit VPS37B)	
XRCC5*	X-ray repair cross-complementing protein 5 (EC 3.6.4.-) (86 kDa subunit of Ku antigen) (ATP-dependent DNA helicase 2 subunit 2) (ATP-dependent DNA helicase II 80 kDa subunit) (CTC box-binding factor 85 kDa subunit) (CTC85) (CTCBF) (DNA repair protein XRCC5) (Ku80) (Ku86) (Lupus Ku autoantigen protein p86) (Nuclear factor IV) (Thyroid-lupus autoantigen) (TLAA) (X-ray repair complementing defective repair in Chinese hamster cells 5 (double-strand-break rejoining))	
YBX1*	Nuclease-sensitive element-binding protein 1 (CCAAT-binding transcription factor I subunit A) (CBF-A) (DNA-binding protein B) (DBPB) (Enhancer factor I subunit A) (EFI-A) (Y-box transcription factor) (Y-box-binding protein 1) (YB-1)	
ATG7	Ubiquitin-like modifier-activating enzyme ATG7 (ATG12-activating enzyme E1 ATG7) (Autophagy-related protein 7) (APG7-like) (hAGP7) (Ubiquitin-activating enzyme E1-like protein)	
C18orf8	Uncharacterized protein C18orf8 (Colon cancer-associated protein Mic1) (Mic-1)	
DOCK4	Dedicator of cytokinesis protein 4	
EIF3B	Eukaryotic translation initiation factor 3 subunit B (eIF3b) (Eukaryotic translation initiation factor 3 subunit 9) (Prt1 homolog) (hPrt1) (eIF-3-eta) (eIF3 p110) (eIF3 p116)	

EIF3E	Eukaryotic translation initiation factor 3 subunit E (eIF3e) (Eukaryotic translation initiation factor 3 subunit 6) (Viral integration site protein INT-6 homolog) (eIF-3 p48)	
EREG	Proepiregulin [Cleaved into: Epiregulin (EPR)]	
FAM161A	Protein FAM161A	
GAS2	Growth arrest-specific protein 2 (GAS-2)	
GATAD1	GATA zinc finger domain-containing protein 1 (Ocular development-associated gene protein)	
GGT5	Gamma-glutamyltransferase 5 (GGT 5) (EC 2.3.2.2) (Gamma-glutamyl transpeptidase-related enzyme) (GGT-rel) (Gamma-glutamyltransferase-like activity 1) (Gamma-glutamyltranspeptidase 5) (Glutathione hydrolase 5) (EC 3.4.19.13) (Leukotriene-C4 hydrolase) (EC 3.4.19.14) [Cleaved into: Gamma-glutamyltransferase 5 heavy chain; Gamma-glutamyltransferase 5 light chain]	
GOLGA4	Golgin subfamily A member 4 (256 kDa golgin) (Golgin-245) (Protein 72.1) (Trans-Golgi p230)	
H1FX	Histone H1x	
HDGF	Hepatoma-derived growth factor (HDGF) (High mobility group protein 1-like 2) (HMG-1L2)	
HDX	Highly divergent homeobox	
HLA-A	HLA class I histocompatibility antigen, A-2 alpha chain (MHC class I antigen A*2)	
HSP90AA4P	Putative heat shock protein HSP 90-alpha A4 (Heat shock 90 kDa protein 1 alpha-like 2) (Heat shock protein 90-alpha D) (Heat shock protein 90Ad)	
MACF1	Microtubule-actin cross-linking factor 1, isoforms 1/2/3/5 (620 kDa actin-binding protein) (ABP620) (Actin cross-linking family protein 7) (Macrophin-1) (Trabeculin-alpha)	
MAN1A1	Mannosyl-oligosaccharide 1,2-alpha-mannosidase IA (EC 3.2.1.113) (Man(9)-alpha-mannosidase) (Man9-mannosidase) (Mannosidase alpha class 1A member 1) (Processing alpha-1,2-mannosidase IA) (Alpha-1,2-mannosidase IA)	
MAP3K5	Mitogen-activated protein kinase kinase kinase 5 (EC 2.7.11.25) (Apoptosis signal-regulating kinase 1) (ASK-1) (MAPK/ERK kinase kinase 5) (MEK kinase 5) (MEKK 5)	
MARCKS	Myristoylated alanine-rich C-kinase substrate (MARCKS) (Protein kinase C substrate, 80 kDa protein, light chain) (80K-L protein) (PKCSL)	
MARCKSL1	MARCKS-related protein (MARCKS-like protein 1) (Macrophage myristoylated alanine-rich C kinase substrate) (Mac-MARCKS) (MacMARCKS)	
MED13L	Mediator of RNA polymerase II transcription subunit 13-like (Mediator complex subunit 13-like) (Thyroid hormone receptor-associated protein 2) (Thyroid hormone receptor-associated protein	

	complex 240 kDa component-like)	
NAA15	N-alpha-acetyltransferase 15, NatA auxiliary subunit (Gastric cancer antigen Ga19) (N-terminal acetyltransferase) (NMDA receptor-regulated protein 1) (Protein tubedown-1) (Tbdn100)	
NCL	Serine/threonine-protein kinase Nek5 (EC 2.7.11.1) (Never in mitosis A-related kinase 5) (NimA-related protein kinase 5)	
NUMA1	Nuclear mitotic apparatus protein 1 (NuMA protein) (Nuclear matrix protein-22) (NMP-22) (SP-H antigen)	
PIFO	Protein pitchfork	
PNMA2	Paraneoplastic antigen Ma2 (40 kDa neuronal protein) (Onconeuronal antigen Ma2) (Paraneoplastic neuronal antigen MM2)	
RBM3	RNA-binding protein 3 (RNA-binding motif protein 3) (RNPL)	
RPL32	60S ribosomal protein L32	
SERBP1	Plasminogen activator inhibitor 1 RNA-binding protein (PAI1 RNA-binding protein 1) (PAI-RBP1) (SERPINE1 mRNA-binding protein 1)	
SETSIP	Protein SETSIP (SET pseudogene protein 18) (SET similar protein) (Similar to SET translocation protein)	
SF3A1	Splicing factor 3A subunit 1 (SF3a120) (Spliceosome-associated protein 114) (SAP 114)	
SF3A2	Splicing factor 3A subunit 2 (SF3a66) (Spliceosome-associated protein 62) (SAP 62)	
SGMS1	Phosphatidylcholine:ceramide cholinephosphotransferase 1 (EC 2.7.8.27) (Medulla oblongata-derived protein) (Protein Mob) (Sphingomyelin synthase 1) (Transmembrane protein 23)	
SNRPB2	U2 small nuclear ribonucleoprotein B" (U2 snRNP B")	
SNTA1	Alpha-1-syntrophin (59 kDa dystrophin-associated protein A1 acidic component 1) (Pro-TGF-alpha cytoplasmic domain-interacting protein 1) (TACIP1) (Syntrophin-1)	
SRRM1	Serine/arginine repetitive matrix protein 1 (SR-related nuclear matrix protein of 160 kDa) (SRm160) (Ser/Arg-related nuclear matrix protein)	
STUB1	E3 ubiquitin-protein ligase CHIP (EC 2.3.2.27) (Antigen NY-CO-7) (CLL-associated antigen KW-8) (Carboxy terminus of Hsp70-interacting protein) (RING-type E3 ubiquitin transferase CHIP) (STIP1 homology and U box-containing protein 1)	
SUGP1	SURP and G-patch domain-containing protein 1 (RNA-binding protein RBP) (Splicing factor 4)	
TMSB10	Thymosin beta-10	
TNNI3	Troponin I, cardiac muscle (Cardiac troponin I)	
TSPAN8	Tetraspanin-8 (Tspan-8) (Transmembrane 4 superfamily member 3) (Tumor-associated antigen CO-029)	
USP9X	Probable ubiquitin carboxyl-terminal hydrolase FAF-X (EC	

	3.4.19.12) (Deubiquitinating enzyme FAF-X) (Fat facets in mammals) (hFAM) (Fat facets protein-related, X-linked) (Ubiquitin thioesterase FAF-X) (Ubiquitin-specific protease 9, X chromosome) (Ubiquitin-specific-processing protease FAF-X)	
VGF	Neurosecretory protein VGF [Cleaved into: Neuroendocrine regulatory peptide-1 (NERP-1); Neuroendocrine regulatory peptide-2 (NERP-2); Antimicrobial peptide VGF[554-577]]	
XRCC6	X-ray repair cross-complementing protein 6 (EC 3.6.4.-) (EC 4.2.99.-) (5'-deoxyribose-5-phosphate lyase Ku70) (5'-dRP lyase Ku70) (70 kDa subunit of Ku antigen) (ATP-dependent DNA helicase 2 subunit 1) (ATP-dependent DNA helicase II 70 kDa subunit) (CTC box-binding factor 75 kDa subunit) (CTC75) (CTCBF) (DNA repair protein XRCC6) (Lupus Ku autoantigen protein p70) (Ku70) (Thyroid-lupus autoantigen) (TLAA) (X-ray repair complementing defective repair in Chinese hamster cells 6)	
ZNF614	Zinc finger protein 614	

Table S4. Comparison of different methods for EV isolation.

Methods	Sample types	Volume	Sample preparation	Over-all Cost	EV Yield	EV Purity	Time	Ref.
Ultracentrifugation (UC)	Culture media	>30 mL	Multi-step processing	High	Low	Low to moderate	Days	1, 7
	Ascitic fluid/Urine							
	Plasma/serum							
Filter method	Culture media	60 mL	Low	Low	Low	Low	Hours	8
Polyethylene glycol (PEG)	Culture media	1-5 mL	Low	Low	Low	Low	Hours	9,10
	Plasma/serum	60-300 µL						
	Ascitic fluid/Urine	1-5 mL						
Antibody-magnetic Beads	Culture media	1mL	Low	Low	Low	Moderate to high	Hours	11
	Plasma/serum	100 µL						
Size-based microfluidic methods	Culture media/urine	1 mL	Low	Moderate	Low	Low	Hours	12-16
	Plasma/serum	100 µL						
ExoTIC device	Culture media	0.5-50 mL	Low	Low	High	High	Hours	
	Plasma/serum	10-500 µL						
	Lavage/urine/ascetic fluids	1-50 mL						

REFERENCES

(1) Thery, C.; Clayton, A.; Amigorena, S.; Raposo, G. Isolation and Characterization of Exosomes from Cell Culture Supernatants and Biological Fluids. *Curr. Prot. in Cell Biol.* **2006**, 3.22.1−3.22.29.

(2) Jensen, K. H.; Valente, A. X.; Stone, H. A. Flow Rate through Microfilters: Influence of the Pore Size Distribution, Hydrodynamic Interactions, Wall Slip, and Inertia. *Physics of Fluids* **2014,** *26*, 052004−052013.

(3) Chen, Q. Enhanced Fluid Flow through Nanopores by Polymer Brushes. *Langmuir* **2014,** *30*, 8119−8123.

(4) Dagan, Z.; Weinbaum, S.; Pfeffer, R. An Infinite-Series Solution for the Creeping Motion through an Orifice of Finite Length. *J. Fluid Mech.* **2006,** *115*, 505−523.

(5) Xu, Y.; Milledge, J. J.; Abubakar, A.; Swamy, R. A. R.; Bailey, D.; Harvey, P. J. Effects of Centrifugal Stress on Cell Disruption and Glycerol Leakage from Dunaliella Salina. *Microalgae Biotechnology* **2015,** *1,* 20−27.

(6) Harrington, W. F.; Kegeles, G. [13] Pressure Effects in Ultracentrifugation of Interacting Systems. *Methods in Enzymology Part D: Enzyme Structure* **1973**, 306−345.

(7) Li, P.; Kaslan, M.; Lee, S. H.; Yao, J.; Z., G. Progress in Exosome Isolation Techniques. *Theranostics* **2017,** *7*.

(8) Heinemann, M. L.; Ilmer, M.; Silva, L. P.; Hawke, D. H.; Recio, A.; Vorontsova, M. A.; Alt, E.; Vykoukal, J. Benchtop Isolation and Characterization of Functional Exosomes by Sequential Filtration. *J. Chromatogr. A* **2014,** *1371*, 125−135.

(9) System Biosciences, L. Methods for Microvesicle Isolation and Selective Removal *US20130337440* **2013**.

(10) Rider, M. A.; Hurwitz, S. N.; Meckes, D. G., Jr. Extrapeg: A Polyethylene Glycol-Based Method for Enrichment of Extracellular Vesicles. *Sci. Rep.* **2016,** *6*, 23978.

(11) Neurauter, A.; Kullmann, A.; Kierulf, B.; Oksvold, M. P.; Pedersen, K. W. Magnetic Beads for Fast and Reproducible Isolation/Characterization of Exosomes Based on Surface Protein Expression. *Poster* **2013**.

(12) Lee, K.; Shao, H.; Weissleder, R.; Lee, H. Acoustic Purification of Extracellular Microvesicles. *ACS Nano* **2015,** *9,* 2321−2327.

(13) Wang, Z.; Wu, H. J.; Fine, D.; Schmulen, J.; Hu, Y.; Godin, B.; Zhang, J. X.; Liu, X. Ciliated Micropillars for the Microfluidic-Based Isolation of Nanoscale Lipid Vesicles. *Lab Chip* **2013,** *13*, 2879−2882.

(14) Davies, R. T.; Kim, J.; Jang, S. C.; Choi, E. J.; Gho, Y. S.; Park, J. Microfluidic Filtration System to Isolate Extracellular Vesicles from Blood. *Lab Chip* **2012,** *12*, 5202−5210.

(15) Wunsch, B. H.; Smith, J. T.; Gifford, S. M.; Wang, C.; Brink, M.; Bruce, R. L.; Austin, R. H.; Stolovitzky, G.; Astier, Y. Nanoscale Lateral Displacement Arrays for the Separation of Exosomes and Colloids Down to 20 Nm. *Nat. Nanotechnol.* **2016,** *11*, 936−940.

(16) Woo, H. K.; Sunkara, V.; Park, J.; Kim, T. H.; Han, J. R.; Kim, C. J.; Choi, H. I.; Kim, Y. K.; Cho, Y. K. Exodisc for Rapid, Size-Selective, and Efficient Isolation and Analysis of Nanoscale Extracellular Vesicles from Biological Samples. *ACS Nano* **2017,** *11*, 1360−1370.